THE JOURNAL OF BIOLOGICAL CHEMISTRY VOL. 283, NO. 48, pp. 33719–33729, November 28, 2008

Regulation of Insulin Granule Turnover in Pancreatic β-Cells by Cleaved ICA512*[S]

Received for publication, June 27, 2008, and in revised form, September 8, 2008 Published, JBC Papers in Press, September 29, 2008, DOI 10.1074/jbc.M804928200

Mirko Trajkovski[‡1], Hassan Mziaut[‡1], Sandra Schubert[‡], Yannis Kalaidzidis[§¶], Anke Altkrüger[‡], and Michele Solimena[‡§‖2]**

*From the [‡]Laboratory of Experimental Diabetology, [‖]Department of Medicine III, and **Center for Regenerative Therapy Dresden, School of Medicine, Dresden University of Technology, Dresden 01307, Germany, the [§]Max Planck Institute of Molecular Cell Biology and Genetics, Dresden 01307, Germany, and the [¶]A. N. Belozersky Institute of Physico-Chemical Biology, Moscow State University, Moscow 119899, Russia*

Insulin maintains homeostasis of glucose by promoting its uptake into cells from the blood. Hyperglycemia triggers secretion of insulin from pancreatic β-cells. This process is mediated by secretory granule exocytosis. However, how β-cells keep granule stores relatively constant is still unknown. ICA512 is an intrinsic granule membrane protein, whose cytosolic domain binds β2-syntrophin, an F-actin-associated protein, and is cleaved upon granule exocytosis. The resulting cleaved cytosolic fragment, ICA512-CCF, reaches the nucleus and up-regulates the transcription of granule genes, including insulin and *ICA512*. Here, we show that ICA512-CCF also dimerizes with intact ICA512 on granules, thereby displacing it from β2-syntrophin. This leads to increased granule mobility and insulin release. Based on these findings, we propose a model whereby the generation of ICA512-CCF first amplifies insulin secretion. The ensuing reduction of granule stores would then increase the probability of newly generated ICA512-CCF to reach the nucleus and enhance granule biogenesis, thus allowing β-cells to constantly adjust production of granules to their storage size and consumption. Pharmacological modulation of these feedback loops may alleviate deficient insulin release in diabetes.

Type 2 diabetes mellitus is a common metabolic disorder, the prevalence of which is rapidly increasing worldwide (1, 2). Excessive food intake and reduced physical activity are mainly responsible for the inability of insulin secretion to meet metabolic demand (3). Discovering ways to ameliorate insulin release is therefore a major goal of diabetes research.

Each β-cell stores ~10^4 insulin secretory granules (4, 5). Less than 1% of the granules are immediately releasable, whereas the remaining must be primed and recruited to membranes before they can undergo exocytosis. This process requires several ATP-, Ca^{2+}-, and phosphatidylinositol 4,5-bisphosphate ($PI(4,5)P_2$)-dependent[3] steps (6, 7). Kinesin and myosin Va drive the ATP-dependent transport of insulin granules toward the cell surface on microtubules and cortical actin microfilaments, respectively (8–11). The meshwork of cortical actin filaments, on the other hand, can inhibit insulin secretion by restricting granule mobility and their access to the plasma membrane (12–14). Despite progress in this area (15), questions remain about how granules dynamically interact with the actin cytoskeleton.

We recently proposed that ICA512 (islet cell autoantigen 512/IA-2) tethers insulin granules to actin microfilaments (16–18). ICA512 is a receptor protein-tyrosine phosphatase family member that lacks phosphatase activity and is mostly expressed in neuroendocrine cells (19–23). Its pro-form is a glycoprotein of 110 kDa that is processed by furin-like convertases during granule maturation (22). This cleavage generates a 65-kDa transmembrane fragment (ICA512-TMF) that in human ICA512 encompasses residues 449–979 (supplemental Fig. 1*A*). The cytoplasmic tail of ICA512-TMF binds to the PDZ domain of β2-syntrophin (16), which in turn interacts with actin microfilaments through utrophin (24). Glucose stimulation may induce the dissociation of ICA512-TMF from β2-syntrophin by affecting the phosphorylation of the latter, hence increasing granule mobility (17).

Ca^{2+}-dependent exocytosis of secretory granules triggers the transient insertion of ICA512-TMF into the plasma membrane (22) and its intracellular cleavage by the Ca^{2+}-activated protease calpain-1 (17). The resulting cleaved cytosolic fragment (ICA512-CCF; residues 659–979) contains the decoy protein-tyrosine phosphatase module flanked by two regions that bind to the PDZ domain of β2-syntrophin (supplemental Fig. 1*A*). ICA512-CCF is targeted to the nucleus, where it enhances the transcription of insulin and other granule genes as well as β-cell proliferation (25–27). Accordingly, $ICA512^{-/-}$ mice display reduced insulin secretion, glucose intolerance, and impaired

* This work was supported by Deutsche Forschungsgemeinschaft SFB655 (Sonderforschungsbereich), Bundesministerium für Bildung und Forschung Grant NBL3, the European Foundation for the Study of Diabetes, the Juvenile Diabetes Research Foundation, and the Max Planck Society (to M. S.) and a MeDDrive Grant from TU Dresden (to M. T.). The costs of publication of this article were defrayed in part by the payment of page charges. This article must therefore be hereby marked "*advertisement*" in accordance with 18 U.S.C. Section 1734 solely to indicate this fact.

[S] The on-line version of this article (available at http://www.jbc.org) contains supplemental Figs. 1–4 and Movies 1 and 2.

[1] Both of these authors contributed equally to this work.

[2] To whom correspondence should be addressed: Fetscherstrasse 74, 01307 Dresden, Germany. Fax: 49-351-4586330; E-mail: michele.solimena@tu-dresden.de.

[3] The abbreviations used are: $PI(4,5)P_2$, phosphatidylinositol 4,5-bisphosphate; TMF, transmembrane fragment; CCF, cleaved cytosolic fragment; GST, glutathione *S*-transferase; GFP, green fluorescent protein; CgB, chromogranin B; HA, hemagglutinin; HG, high glucose; HK, high KCl; HGHK, high glucose and high KCl; SI, insulin stimulation index.

regeneration of β-cells (25, 28). Moreover, overexpression of ICA512 in mouse insulinoma MIN6 cells increases the number of granules as well as the content, half-life, and stimulated secretion of insulin (29). A mechanistic explanation for these findings, however, is lacking. Here we demonstrate that ICA512-CCF, in addition to granule biogenesis, enhances insulin secretion.

EXPERIMENTAL PROCEDURES

Islet Isolations and Cell Cultures—Pancreatic islets were isolated from 15–17-week-old *ICA512*$^{-/-}$ mice (26) and wild type littermates, as described (30), and then kept for 24 h in culture prior to the experiment. INS-1-derived INS-1E and tetracycline-inducible INS-r3 cells (31, 32) were gifts from C. Wollheim (University of Geneva, Geneva, Switzerland) and were grown as described (33). Wild type and transfected INS-1E cells and pancreatic islets were incubated for 60 min in resting buffer (0 mM glucose and 5 mM KCl) and then for 105 min in fresh resting or stimulating buffer (25 mM glucose and 55 mM KCl), as described (17, 27). Calpeptin and cycloheximide (Calbiochem, Gibbstown, NJ) were added in the last 15 min of the preincubation and left until cells were harvested.

cDNA Constructs—The following constructs were described: human ICA512-GFP, ICA512-CCF-GFP, and ICA512-HA3 (17, 27); GST-ICA512-(601–979), GST-ICA512-(663–979), GST-ICA512-(700–959), GST-ICA512-(700–979), GST-ICA512^{extracellular}, and GST-ICA512-(800–979) (16); ICA512-(601–979)-His (17); ICA512-CCF$^{AD/DA}$-GFP (26); and mouse GFP-β2-syntrophin (34). ICA512-CCF-HA3 and HA3-ICA512-CCF were generated by subcloning the cDNA encoding residues 659–979 of human ICA512 as a KpnI-XbaI insert into pMoHa3 (a gift from M. Suchanek and C. Thiele, Max Planck Institute of Cell Biology and Genetics, Dresden, Germany) or as a BglII-EcoRI insert into pN3HA (Clontech, Mountain View, CA), respectively. For tetracycline-inducible expression of ICA512-CCF-GFP, the corresponding cDNA (27) was subcloned as a BamHI/XbaI insert between the tetracycline-operator-*tk*-minimal promoter and the SV40 poly(A) in a vector derived from the tetracycline-*tk*-luc plasmid (35). Subsequently, the tetracycline-*tk*-ICA512-CCF-GFP-pA cassette was cloned between chicken β-globin insulators in a vector kindly provided by K. Anastassiadis (Biotec, TUD, Dresden, Germany). The mouse cDNA of the granule cargo chromogranin B (CgB; a gift from W. Huttner, Max Planck Institute of Cell Biology and Genetics) was fused in frame at the 5′-end of the cDNA for monomeric Red Fluorescent Protein 1 (36) (mRFP1; Planetgene, Menlo Park, CA). All clones were generated using conventional procedures and verified by DNA sequencing.

Cell Transfections—INS-1E cells were electroporated using the Amaxa nucleoporator with a transfection efficiency of ~60–70%, as described (27). Generation of stable GFP- and ICA512-CCF-GFP INS-1 cell clones was described (27). INS-r3 cells expressing the reverse tetracycline-dependent *trans*-activator were transiently transfected with ICA512-CCF-GFP in the tetracycline-*tk*-luc-derived plasmid. Expression of ICA512-CCF-GFP was induced by exposure to 500 ng/ml doxycycline for 16, 24, 36, or 48 h. CgB-mRFP1 INS-1 clones were selected for puromycin resistance and further screened by fluorescence microscopy and immunoblotting for expression of the transgene.

Cell Extracts and Western Blots—Purified mouse islets and INS-1E cells were washed with ice-cold PBS and extracted in lysis buffer (10 mM Tris-HCl, pH 8.0, 140 mM NaCl, 1% Triton X-100, 1 mM EDTA, 1 mM phenylmethylsulfonyl fluoride, 1% phosphatase inhibitors (Calbiochem), and 1% protease inhibitor mixture (Sigma, St. Louis, MO) at 4 °C. Protein measurements and immunoblottings were performed as described (27) using the following primary antibodies: mouse monoclonal antibodies mICA512 (37), mICA512-HM1 (26), anti-γ-tubulin (Sigma), and anti-GFP (Clontech); anti-ICA512ecto (22), anti-carboxypeptidase E/H (CPE) (Chemicon, Temecula, CA), and goat anti-GFP (a gift from D. Drechsel, Max Planck Institute of Cell Biology and Genetics). Chemiluminescence was developed and quantified as described (27).

Immunoprecipitations—INS-1E cells were transiently or stably transfected with one or more of the following constructs: GFP, *ICA512-CCF-GFP*, GFP-β2-syntrophin, *ICA512-CCF-HA3*, and *HA3-ICA512-CCF*. Protein extracts in 20 mM Tris-HCl at pH 8.0, 200 mM NaCl, 1% Triton X-100, 0.1% SDS, 1 mM EDTA, 1 mM phenylmethylsulfonyl fluoride, 1% phosphatase inhibitors (Calbiochem), and 1% protease inhibitor mixture (Sigma) were incubated overnight at 4 °C with one of the following antibodies: goat anti-GFP, rabbit anti-ICA512ecto, goat or rabbit IgGs (Sigma), followed by incubation with protein G-Sepharose (GE Healthcare, Piscataway, NJ) for 90 min. The beads were then washed 10 times and loaded on 8–10% SDS-PAGE followed by Western blot with one of the following mouse antibodies: anti-ICA512, anti-GFP (Clontech), anti-β2-syntrophin (a gift from S. Froehner and M. Adams, University of Washington, Seattle), anti-HA, and anti-γ-tubulin.

Pull-down Assays—ICA512-(601–979)-His or β2-syntrophin-His in pET28a (16) were *in vitro* transcribed and translated with the T7/coupled transcription-translation kit (Promega, Madison, WI). GST-ICA512-(601–979) or GST were expressed in bacteria as described (17, 26). [^{35}S]Methionine-β2-syntrophin-His was incubated overnight at 4 °C in GST binding buffer (240 mM NaCl, 50 mM Tris, pH 8, 0.25% Nonidet P-40, 0.15% SDS, 1 mM dithiothreitol, and 1 mM phenylmethylsulfonyl fluoride) with GST fusion proteins or GST alone coupled to glutathione-Sepharose beads (GE Healthcare). Beads were washed 10 times with binding buffer and eluted with 10 mM reduced glutathione. Eluted proteins were subjected to SDS-PAGE and analyzed by autoradiography.

Immunocytochemistry—Labeling of transfected or nontransfected INS-1E cells was performed as described (27). The following primary and secondary antibodies were used: mouse anti-insulin (Sigma), rabbit anti-TGN38 (BD Transduction Laboratories, Franklin Lakes, NJ), Alexa^{568}-conjugated goat anti-mouse or Alexa^{488}-conjugated goat-anti-rabbit IgGs and phalloidin-rhodamine (Molecular Probes, Inc., Eugene, OR). Nuclei were counterstained with 4′,6-diamidino-2-phenylindole (Sigma), and coverslips were mounted with Mowiol (Calbiochem). Images of 0.5-μm optical sections were acquired at room temperature with an inverted confocal microscope Zeiss

Axiovert 200M equipped with a Plan-Apochromat ×63 oil objective, numerical aperture 1.4, a Zeiss LSM510 scan head with photomultiplier tubes, and the software Zeiss LSM 510 AIM version 4 (Zeiss, Göttingen, Germany).

RNA Interference—For knockdown of rat ICA512 and β2-syntrophin, the following oligonucleotides were used to generate silencing hairpin in the pGENE-CLIP U1 cassette system (Promega) according to the manufacturer's instructions: ICA512 short hairpin RNA oligo1, 5′-TCTCGCGCCATCATTCGAAACAATTCAAGAGATTGTTTCGAATGATGGCGCCT-3′; ICA512 short hairpin RNA oligo2, 5′-TCTCGCAGTACAAGCAGATGTAATTCAAGAGATTACATCTGCTTGTACTGCCT-3′, as previously described (25); β2-syntrophin short hairpin RNA oligo1, 5′-TCTCGTAGCTATCCACACCAACATATTCAAGAGATATGTTGGTGTGGATAGCTACCT-3′. Single or double transfections of INS-1E cells with pGENE-ICA512 and pGENE-β2-syntrophin by electroporation were performed as described (27), using 4 or 3 μg of each plasmid for single or double transfection, respectively. Cells were stimulated and harvested 4 days after transfection, and knockdown of ICA512 and β2-syntrophin was determined by real time PCR and Western blot, as described (27).

Insulin Radioimmune Assay—Insulin secretion was assessed as a ratio between insulin in the medium and the cell insulin content. After stimulation, 25–30 purified pancreatic islets were resuspended in fresh resting or stimulating medium and sonicated for 4 min. INS-1E cells were extracted overnight in 3:1:0.06 volumes of ethanol, H_2O, and 37% HCl at −20 °C. Following centrifugation, insulin in islet cells and in the medium was measured with the Sensitive Rat Insulin RIA kit (Linco Research, St. Charles, MO). The insulin stimulation index was calculated as follows: secreted/total insulin in stimulated conditions *versus* secreted/total insulin in resting conditions.

Total Internal Reflection Fluorescence Microscopy (TIRFM)—Images of INS-1 cells stably expressing mouse CgB-mRFP1 were acquired with a Roper Scientific MicroMAX512BFT charge-coupled device camera with a Zeiss Axiovert 200M microscope equipped with an argon laser and a Zeiss ×100/1.45 numerical aperture Plan-FLUAR objective and a ×1.6 optovar. The microscope was outfitted with a dual port total internal reflection fluorescence condenser (Till Photonics, Gräfelfing, Germany). Prior to imaging, cells grown in an open chamber were incubated in resting media and transferred onto a thermostat-controlled (37 °C) stage. CgB-mRFP1$^+$ granules in GFP$^+$ cells were visualized by excitation of mRFP1 at 488 nm using filter sets for tetramethylrhodamine isothiocyanate emission (Chroma Technology Corp., Rockingham, VT). Images were collected using the software MetaMorph (Molecular Devices, Sunnyvale, CA) at the speed of 2 frames/s with an exposure time of 100 ms, for a total of 4 min (480 frames) for each movie (supplemental Movies 1 and 2). Automated image analysis was performed with the MotionTracking/Kalaimoscope software (Transinsight GmbH, Dresden, Germany), as described (38). The background of nonvesicular fluorescence was subtracted, and the granules were fitted by analytical function as described (38). The accuracy of granule center definition was estimated from the mean square displacement (*i.e.* the average of squared displacements) and found equal to 60 nm. The jitter of center definition was suppressed by smoothing the tracks with a sliding window (±2 frames). Statistical data for granule density were obtained from 10 films. The total number of tracked CgB-mRFP1$^+$ granules in GFP$^+$ and ICA512-CCF-GFP$^+$ cells was 779 and 888, respectively. Speed was measured between every two sequential frames, and the total number of speed measurements in GFP$^+$ and ICA512-CCF-GFP$^+$ cells was 13,332 and 14,828, respectively.

Statistics and Graphics—Statistical analyses were performed as previously described (26, 27). The *error bars* show S.D. values from at least three independent experiments. Histograms were prepared with Microsoft Excel (Microsoft, Redmond, WA).

RESULTS

ICA512 Cleavage Regulates Exocytosis—We used several approaches to test whether the calpain-mediated cleavage of ICA512-TMF affects insulin secretion from INS-1E cells stimulated with 25 mM glucose (HG) and 55 mM KCl (HK). INS-1E cells were used, since they respond better to glucose than the parental INS-1 cells (31). First, ICA512-TMF cleavage was prevented with the calpain inhibitor calpeptin. As shown for INS-1 cells, calpeptin reduced the cleavage of ICA512-TMF in INS-1E cells by ~70% (17, 27) (supplemental Fig. 1*B*). Calpeptin also inhibited insulin release from HGHK-stimulated mouse pancreatic islets and INS-1E cells (Fig. 1, *A* and *B*).

To test if this reduction resulted from the diminished cleavage of ICA512-TMF, we analyzed insulin secretion from *ICA512*$^{-/-}$ islets. Consistent with previous studies, the insulin stimulation index (SI) of untreated islets from *ICA512*$^{-/-}$ mice was 58 ± 8.7% lower than in *ICA512*$^{+/+}$ islets (28) (Fig. 1*A*). Strikingly, calpeptin did not further decrease insulin secretion from *ICA512*$^{-/-}$ islets, indicating that calpain-1-mediated cleavage of ICA512-TMF regulates insulin secretion (Fig. 1*A*). Accordingly, both transient and stable overexpression of ICA512-GFP in INS-1E cells enhanced insulin release in a dose-dependent and calpeptin-sensitive fashion (Fig. 1*B*).

Next, we investigated whether cleavage of ICA512-TMF affects insulin secretion by promoting insulin gene expression and granule biogenesis. Block of protein synthesis with 100 μM cycloheximide did not prevent calpeptin from inhibiting stimulated insulin release (Fig. 1*C*). Depolarization of β-cells with HK alone triggers Ca^{2+} entry, granule exocytosis, and cleavage of ICA512-TMF (17, 27) but not the rapid biosynthesis of preproinsulin and pro-ICA512 (17, 27, 39) (supplemental Fig. 1*B*). Notably, stimulation with HK increased insulin secretion ~5-fold from *ICA512*$^{+/+}$ islets but not from ICA512$^{-/-}$ islets (Fig. 1*D*). Moreover, HK-stimulated insulin secretion was calpeptin-sensitive in ICA512$^{+/+}$ islets but not in *ICA512*$^{-/-}$ islets (Fig. 1*D*). Taken together, these data suggest that cleavage of ICA512-TMF promotes insulin secretion independently of granule biogenesis.

ICA512-CCF Enhances Insulin Secretion—We next evaluated whether ICA512-CCF directly affects insulin secretion. We found that overexpression of ICA512-CCF fused to

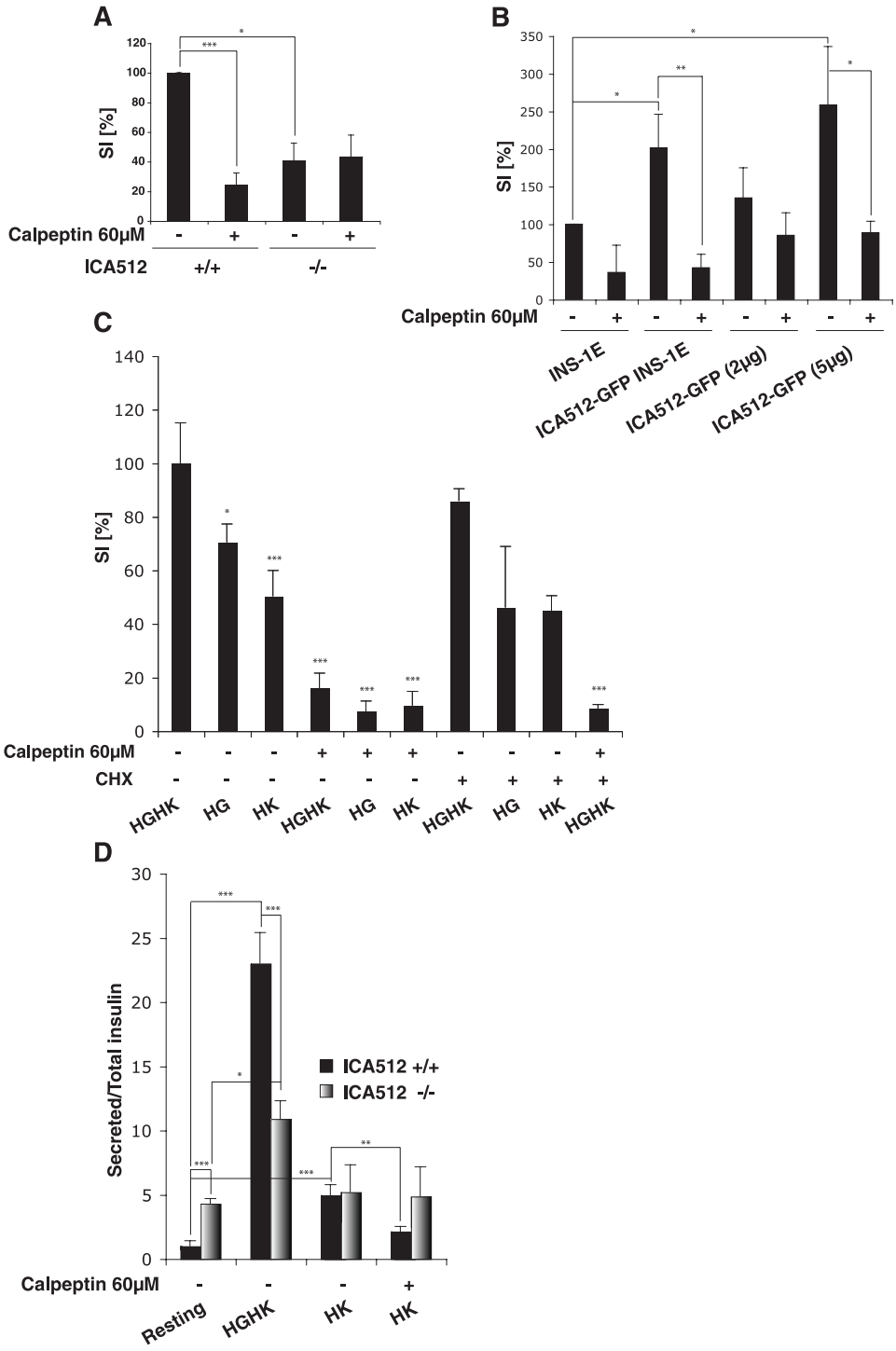

FIGURE 1. **Calpain-1-mediated cleavage of ICA512 regulates insulin secretion.** *A*, SI of *ICA512*$^{+/+}$ *ICA512*$^{-/-}$ mouse pancreatic islets stimulated with 25 mM glucose and 55 mM KCl (HGHK) for 90 min in the presence (+) or absence (−) of 60 μM calpeptin. The SI of *ICA512*$^{+/+}$ islets equals 100%. *B*, SI of INS-1E cells nontransfected or transfected stably or transiently with 2 or 5 μg *ICA512-GFP* and then stimulated with HGHK for 120 min in the presence (+) or absence (−) of 60 μM calpeptin. The SI of nontransfected INS-1E cells equals 100%. *C*, SI of INS-1E cells stimulated either with HG, HK, or both. Cells were treated with or without 60 μM calpeptin, 100 μM cycloheximide (*CHX*), or both. The SI of cells stimulated with HGHK equals 100%. *D*, ratio of secreted *versus* total insulin of *ICA512*$^{+/+}$ (*black columns*) or *ICA512*$^{-/-}$ (*gray columns*) mouse islets kept at rest or stimulated with HGHK or HK and treated with or without 60 μM calpeptin. The ratio in resting, untreated *ICA512*$^{+/+}$ islets equals 1. *Error bars*, mean ± S.D. All results are from at least three independent experiments except *D*, which is from two independent experiments performed in triplicate. *, $p < 0.05$; **, $p < 0.01$; ***, $p < 0.005$.

green fluorescent protein (ICA512-CCF-GFP), but not GFP alone, increased stimulated insulin release from INS-1E cells in a dose-dependent fashion (Fig. 2*A*). Strikingly, calpeptin did not inhibit insulin secretion from cells expressing ICA512-CCF, whereas it decreased secretion by 77 ± 5.3 and 75 ± 13.0% from control and GFP-expressing cells, respectively (Fig. 2*A*). These data indicate that ICA512-CCF enhances granule exocytosis directly and not through the activity of other calpain-sensitive proteins.

To further investigate its relationship with insulin secretion, ICA512-CCF-GFP was expressed in a tetracycline-inducible fashion in INS-r3 cells (32). ICA512-CCF-GFP was first detectable 16 h after doxycycline treatment and maximally expressed after 24 h (Fig. 2*B*). Its initial appearance correlated with a reduction of endogenous ICA512-TMF levels, whereas later the expression of both pro-ICA512 and ICA512-TMF increased, consistent with the ability of ICA512-CCF to promote *ICA512* transcription (26). In parallel with the expression of ICA512-CCF-GFP, insulin secretion increased by 65 ± 6.54%, before an increase in insulin content was apparent (Fig. 2, *C* and *D*). Further evidence that ICA512-CCF enhances insulin secretion independently from promoting gene transcription was obtained by expressing the ICA512-CCF$^{AD/DA}$-GFP mutant. This mutant is endowed with tyrosine phosphatase activity because of the replacement of Ala^{877} and Asp^{911} with Asp and Ala, respectively (40). Unlike ICA512-CCF-GFP, ICA512-CCF$^{AD/DA}$-GFP is not enriched in the nucleus and does not enhance gene transcription (26). Nevertheless, ICA512-CCF$^{AD/DA}$-GFP stimulated insulin secretion similarly to ICA512-CCF-GFP (Fig. 2*E*).

Analysis by confocal microscopy showed that overexpression of ICA512-CCF-GFP altered the intracellular distribution of insulin granules (Fig. 3, *A* and *B*). In INS-1E cells expressing ICA512-CCF-GFP, insulin immunoreactivity at the cell periphery was reduced in comparison with control and GFP-expressing cells (Fig. 3, *A*–*C*). Conversely, the insulin labeling was increased throughout the cytoplasm and especially in the

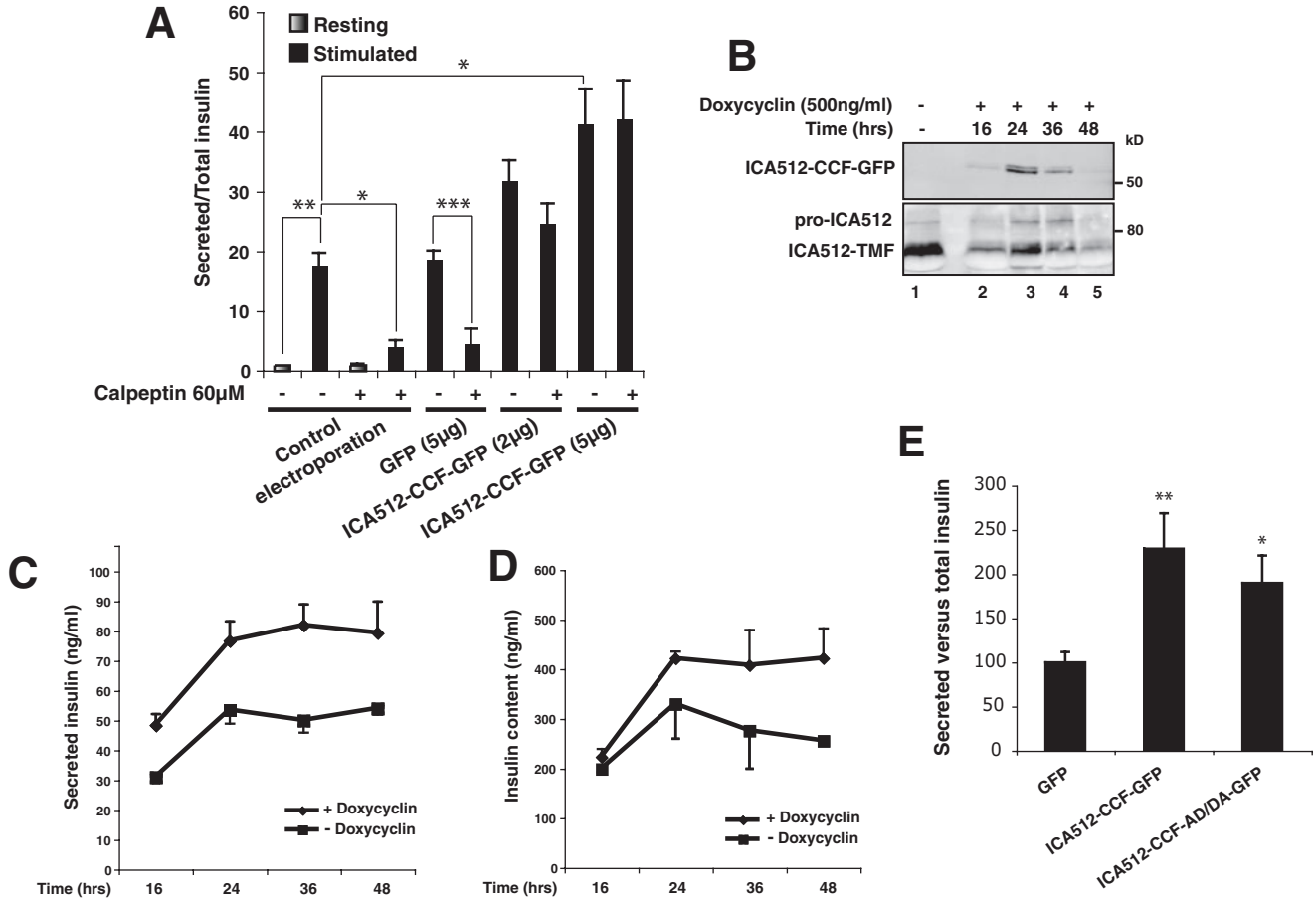

FIGURE 2. **ICA512-CCF stimulates insulin secretion.** *A*, ratio of secreted *versus* total insulin from INS-1E cells nontransfected or transiently transfected with 5 μg of *GFP* or 2 and 5 μg of *ICA512-CCF-GFP* plasmids. Cells were kept at rest or stimulated with HGHK and treated with or without 60 μM calpeptin. The ratio in electroporated, resting INS-1E cells equals 1. *B*, Western blots with anti-GFP (*top*) or anti-ICA512 (*bottom*) antibodies on total protein extracts from INS-r3 cells transiently transfected with tetracycline-inducible *ICA512-CCF-GFP*. Cells were treated with or without 500 ng/ml doxycyclin for the indicated time intervals. *C* and *D*, insulin secretion (*C*) and content (*D*) of INS-r3 cells treated as in *B*. Results in *C* and *D* are from three independent experiments, each in triplicate. *E*, ratio of secreted *versus* total insulin in INS-1 cells expressing GFP, ICA512-CCF-GFP, or ICA512-CCF$^{AD/DA}$-GFP. *Error bars* in *A*, *C*, and *D* show mean ± S.D. The results are from at least three independent experiments performed in triplicate. *, $p < 0.05$; **, $p < 0.01$; ***, $p < 0.005$.

Golgi region (Fig. 3*B* and supplemental Fig. 2*A*). The depletion of peripheral granules in ICA512-CCF-GFP cells was prevented by the co-expression of tetanus toxin light chain, which blocks exocytosis, but not by the inactive tetanus toxin light chain mutant (Fig. 3*D*) (data not shown). Peripheral granules were also diminished in cells expressing ICA512-CCF N-terminally tagged with a triple HA epitope (HA3-ICA512-CCF; supplemental Fig. 2*C*). Similar to ICA512-CCF-GFP, HA3-ICA512-CCF was enriched in the nucleus and increased insulin immunoreactivity in the Golgi region and insulin secretion (supplemental Fig. 2, *B* and *C*). Overall, depletion of insulin at the cell periphery together with its increased levels in the early secretory pathway are consistent with ICA512-CCF having the dual role of enhancing insulin secretion while promoting granule biogenesis.

ICA512-CCF Increases Granule Mobility—ICA512-CCF could increase granule exocytosis by affecting the integrity of the cortical actin cytoskeleton. However, staining of F-actin with phallodin did not reveal gross alterations of the actin network in cells expressing ICA512-CCF-GFP in comparison with GFP cells (supplemental Fig. 3*A*). Another mechanism for enhancing insulin secretion is the mobilization of granules, since it increases their probability to approach the plasma membrane. β-Cell granules exposed to low glucose levels (<5 mM) display mainly short oscillatory movements (<2–3-vesicle diameter), whereas exposure to stimulatory glucose levels (>5 mM) increases their excursions to several micrometers (41). To test whether ICA512-CCF promotes insulin secretion by affecting the granule mobility and/or density near (≤200 nm from) the plasma membrane, we used total internal reflection fluorescence microscopy. For this purpose, INS-1 cells stably transfected with the granule cargo chromogranin B tagged with monomeric red fluorescent protein 1 (*CgB-mRFP1*) were transiently co-transfected with *GFP* or *ICA512-CCF-GFP* (Fig. 4, *A–F*, and supplemental Movies 1 and 2). Co-localization of CgB-mRFP1 with insulin granules was verified by confocal microscopy (supplemental Fig. 3*B*). Computer-assisted analysis with the MotionTracking/Kalaimoscope software, which allows automated particle tracking, revealed a density of 28 ± 9 CgB-mRFP1$^+$ granules/100 μm^2 in *GFP/CgB-mRFP1*-INS1 cells compared with 11 ± 2.6 CgB-mRFP1$^+$ granules/100 μm^2 ($p < 0.005$) in *ICA512-CCF-GFP/CgB-mRFP1*-INS-1 cells in resting conditions (Fig. 4, *A–D* and *G*, and supple-

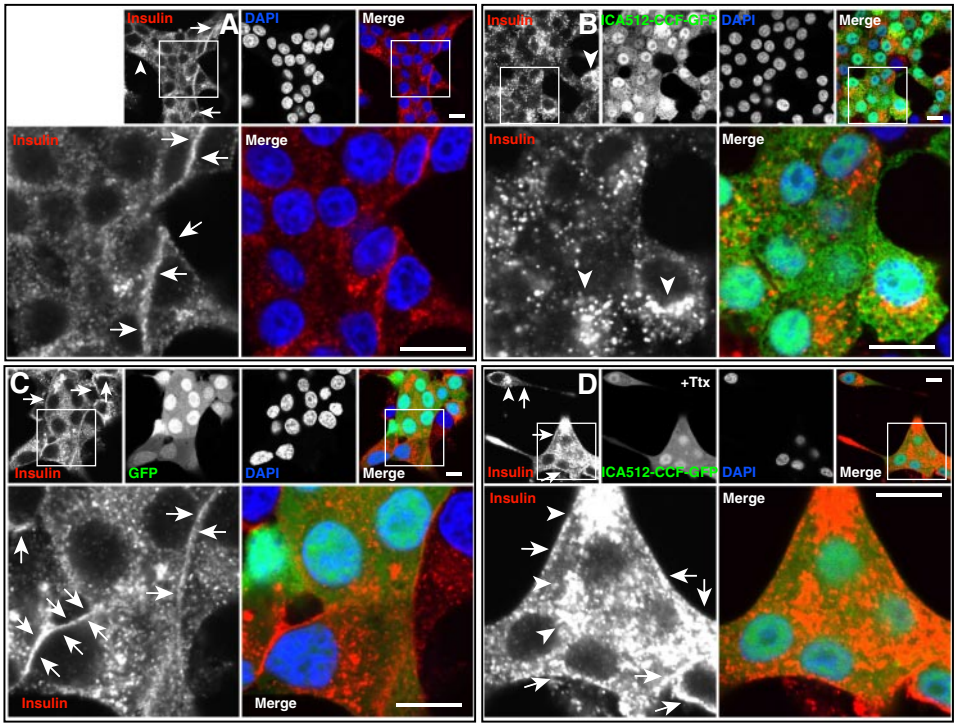

FIGURE 3. **Intracellular distribution of insulin secretory granules is altered in INS-1 cells overexpressing ICA512-CCF.** *A–D*, confocal *z*-sections (0.5 μm) of native INS-1E cells immunolabeled with anti-insulin antibody (*pseudored*). Nuclei were counterstained with 4′,6-diamidino-2-phenylindole (*DAPI*; *pseudoblue*). The *arrows* and *arrowheads* point to the accumulation of insulin immunoreactivity in proximity of the plasma membrane and the perinuclear region, respectively. In *B–D*, cells were transiently transfected with 5 μg of *ICA512-CCF-GFP* (*B* and *D*) or *GFP* (*C*) (*pseudogreen*). In *D*, cells were co-transfected with tetanus toxin light chain, as described (27). *Bars* (*F–I*), 10 μm.

mental Movies 1 and 2). Consistent with the data from confocal microscopy (Fig. 3), these findings demonstrate that ICA512-CCF reduces the density of insulin granules in the cell cortex.

Importantly, the decreased granule density in ICA512-CCF-GFP cells correlated with an increased granule mobility. Indeed, automated particle tracking showed that the mean speed of CgB-mRFP1$^+$ granules in resting *ICA512-CCF-GFP*/*CgB-mRFP1*-INS1 cells was increased relative to resting *GFP*/*CgB-mRFP1*-INS1 (0.113 μm s^{-1} *versus* 0.069 μm s^{-1}, $p = 0.003$) (Fig. 4, *E*, *F*, and *H*).

To gain further insight into the effect of ICA512-CCF on the dynamics of cortical granules, the averaged mean square displacement of CgB-mRFP1$^+$ vesicles was plotted against time. In *ICA512-CCF-GFP*/*CgB-mRFP1*-INS1 cells, the mean square displacement of CgB-mRFP1$^+$ granules showed an almost linear dependence (Fig. 4*I*). This behavior arose from frequent and random changes in the direction of the granules and is characteristic of vesicles whose motion is not constrained (42). Conversely, in *GFP*/*CgB-mRFP1*-INS1 cells, the mean square displacement of CgB-mRFP1$^+$ granules showed a linear dependence for <4 s before curve abatement (Fig. 4*I*). This pattern is characteristic of vesicles caged by the neighboring cytoskeleton network. These data directly prove that ICA512-CCF enhances the motility of granules.

ICA512-CCF and ICA512-TMF Form Homodimers—How does ICA512-CCF enhance granule mobility? Pull-down assays and structural studies have previously shown that the phosphatase-like domain of ICA512 forms a homodimer *in vitro* and in transfected fibroblasts (43, 44) (available on the World Wide Web). Thus, we asked whether ICA512-CCF binds to ICA512-TMF on granule membranes. In support of this hypothesis, we found that ICA512-CCF-GFP was specifically co-immunoprecipitated with endogenous ICA512-TMF using an antibody directed against the ICA512-TMF ectodomain but not with control IgG (Fig. 5*A*). Notably, less ICA512-TMF was detected in the input and immunoprecipitates from ICA512-CCF-GFP cells than from GFP cells (Fig. 5*A*). This reduction is consistent with the increased granule exocytosis, and thereby cleavage of ICA512-TMF in cells that overexpress ICA512-CCF-GFP. Moreover, endogenous ICA512-CCF was co-immunoprecipitated with an anti-GFP antibody from stimulated, but not from resting, INS-1E cells expressing ICA512-GFP (Fig. 5*B*) (data not shown).

ICA512-CCF Displaces ICA512-TMF from β2-Syntrophin—We had previously shown that also β2-syntrophin binds to the cytoplasmic tail of ICA512-TMF and proposed that this association links granules to the cortical actin cytoskeleton (16, 17). Binding of β2-syntrophin could also protect ICA512-TMF from being cleaved by calpain, at least *in vitro* (17). Accordingly, we found that overexpression of GFP-β2-syntrophin increased ICA512-TMF levels in both resting and stimulated INS-1E cells (Fig. 6*A*). Phosphorylation of β2-syntrophin at multiple sites accounts for its detection as a ladder by immunoblotting (17, 46).[4] We also found that ICA512-TMF was co-immunoprecipitated with GFP-β2-syntrophin from extracts of INS-1E cells kept in resting buffer or stimulated in the presence of calpeptin but not from stimulated cells (Fig. 6*B*). We wonder therefore whether ICA512-CCF generated in response to stimulation could disrupt the ICA512-TMF·β2-syntrophin complex by binding to either protein and thus release granules from the cortical cytoskeleton. Thus, we tested whether homodimerization of ICA512 interferes with the binding to ^{35}S-labeled β2-syntrophin-His in pull-down assays. Increasing recovery of ICA512-(601–979)-His with GST-ICA512-(601–979) proportionally correlated with a decreased interaction of

[4] S. Schubert, J. Ouwendijk, S. Mohammed, K. P. Knoch, M. Jager, A. Altkrüger, C. Wegbrod, Adams, E. Marvin, Y. Kim, Froehner, C. Stanley, Jensen, O. Nørregaard, Y. Kalaidzidis, and M. Solimena, manuscript in preparation.

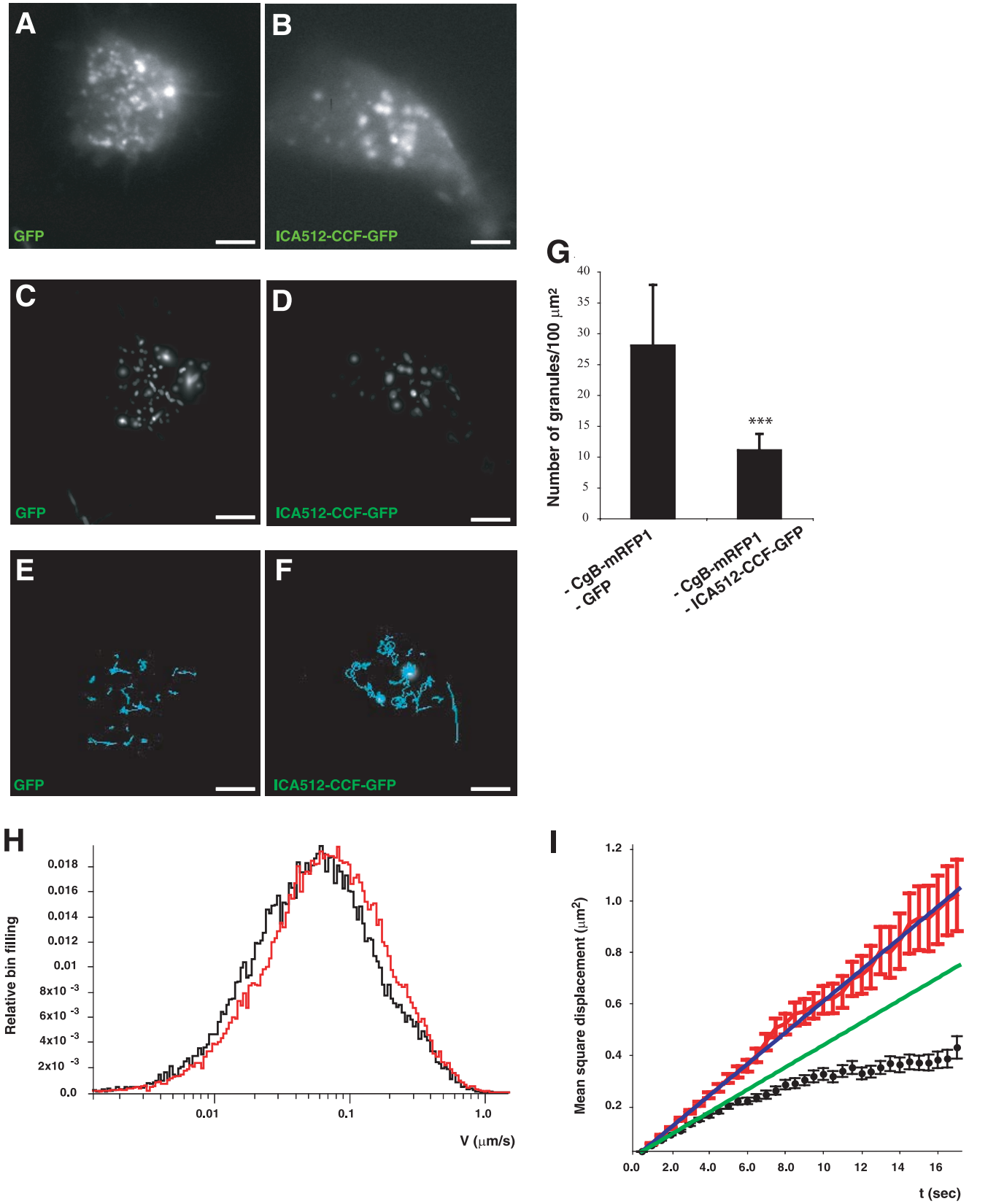

FIGURE 4. **ICA512-CCF increases granule motility.** *A–F*, frames from TIRFM movies tracking the motion of CgB-mRFP1$^+$ granules in resting INS-1 cells expressing GFP (*A*, *C*, and *E*) (supplemental Movie 1) or ICA512-CCF-GFP (*B*, *D*, and *F*) (supplemental Movie 2). *A* and *B* show raw images, whereas *C* and *D* show the tracked granules, as recognized by the MotionTracking/Kalaimoscope software. In *E* and *F*, the motion of individual CgB-mRFP1$^+$ granules tracked for 50 s is displayed by a *blue line*. *G*, density of granules in resting INS-1 cells expressed as number of granules/100 μm^2. *H* and *I*, mean speed velocity (*H*) and square displacement (*I*) of CgB-mRFP1$^+$ granules in resting INS-1 cells expressing GFP (*black traces*) or ICA512-CCF-GFP (*red traces*). In *H*, the histogram bins were sampled uniformly in the logarithmic scale to better present the distribution difference at low speed. The sum of all bins equals 1 for both histograms. In *I*, the *green* and *blue lines* show the weighted linear fit of the three initial mean square displacement points. Bars, 5 μm.

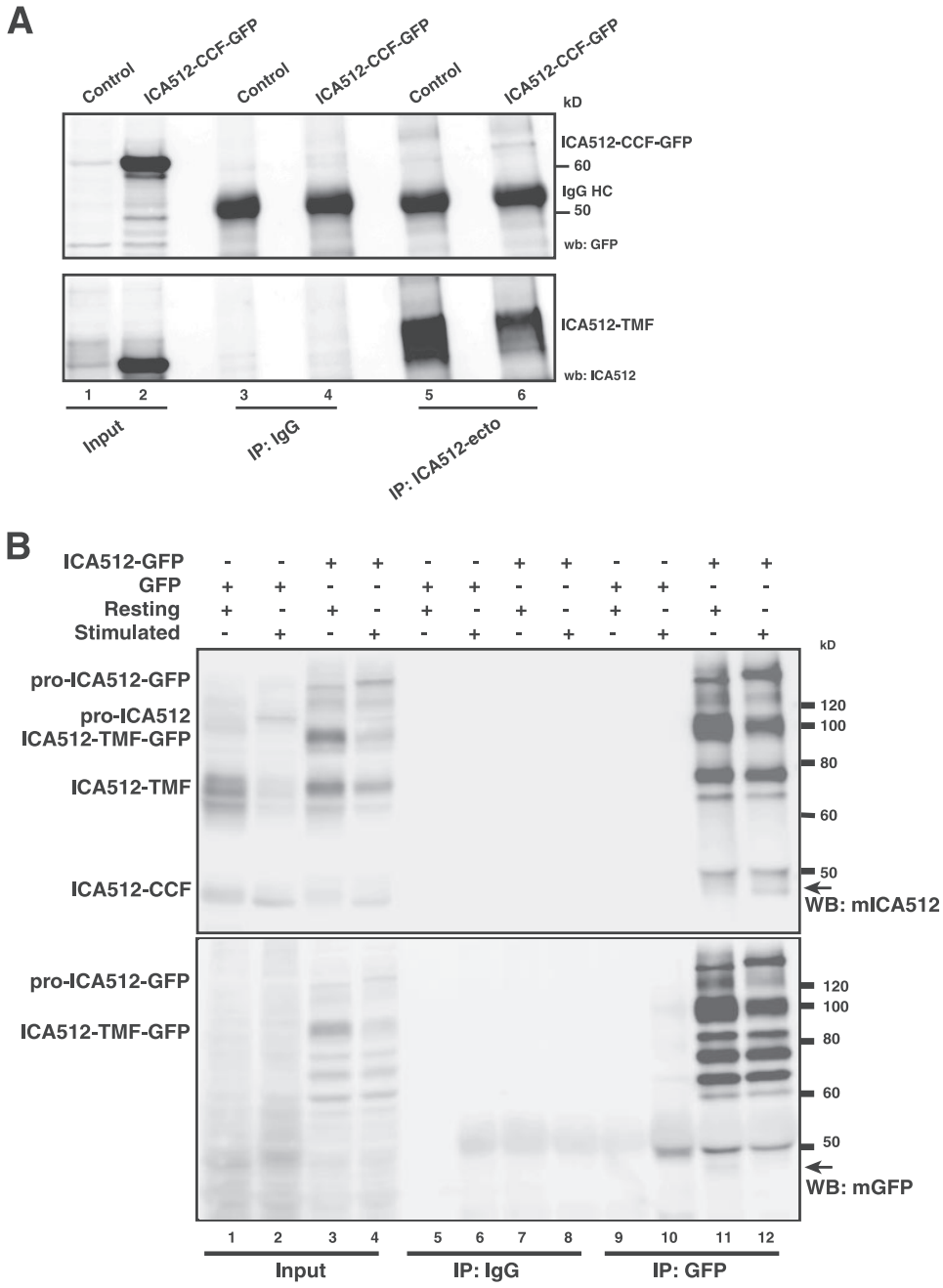

FIGURE 5. **ICA512-CCF dimerizes with ICA512-TMF.** *A*, Western blots with mouse anti-GFP (*top*) or anti-ICA512 (*bottom*) antibodies on total protein extracts (*lanes 1* and *2*) or on immunoprecipitates (*IP*) with control (*lanes 3* and *4*) or rabbit anti-ICA512^{ecto} (*lanes 5* and *6*) immunoglobulins from INS-1E transfected with 5 μg of GFP or *ICA512-CCF-GFP*. *B*, Western blots (*WB*) with mouse anti-ICA512-HM1 (26) (*top*) or anti-GFP (*bottom*) antibodies on cytosolic protein extracts (*lanes 1–4*) or immunoprecipitates with goat control (*lanes 5–8*) or anti-GFP (*lanes 9–12*) immunoglobulins from resting or HGHK-stimulated INS-1E cells. Cells were transfected with 5 μg of GFP or *ICA512-GFP*.

GST-ICA512-(601–979) with ^{35}S-labeled β2-syntrophin-His (Fig. 6*C*).

To verify whether the ICA512-TMF·β2-syntrophin complex regulates granule retention and exocytosis, we further monitored insulin secretion from cells in which the expression of either protein was altered. As expected, knockdown of rat ICA512 decreased stimulated insulin secretion (Fig. 6*D*). Knockdown of rat β2-syntrophin also reduced the insulin stimulation index to 34% ± 1.0 compared with control cells (Fig. 6*D*). These effects were specific, since they could be largely rescued by overexpressing human ICA512-GFP and mouse GFP-β2-syntrophin (supplemental Fig. 4, *A* and *B*). Simultaneous knockdown of both proteins decreased insulin secretion even more (Fig. 6*D*). Conversely, overexpression of GFP-β2-syntrophin increased the insulin stimulation index by 258 ± 80%, and most importantly, this increase was abolished by knockdown of ICA512 (Fig. 6*D*). Likewise, knockdown of β2-syntrophin reduced stimulated insulin secretion from ICA512-GFP-overexpressing cells (Fig. 6*D*). Taken together, these results demonstrate that the ICA512-TMF·β2-syntrophin complex regulates granule retention and exocytosis and that its disruption by ICA512-CFF increases insulin secretion.

DISCUSSION

In this study, we demonstrate that the ICA512-TMF·β2-syntrophin complex regulates turnover of insulin granules and insulin secretion by restraining their motility. Consistent with previous findings (28), we show that the basal insulin release of ICA512$^{-/-}$ islets is increased, whereas their stimulated insulin release is diminished, thereby accounting for the reduction of the insulin stimulation index. A similar reduction of the insulin stimulation index was observed upon the independent knockdown of ICA512 or β2-syntrophin in rat INS-1E cells, supporting the idea that the two proteins act in concert in regulating insulin secretion. Our previous and more recent data (17)[4] indicate that β-cell stimulation alters the phosphorylation of β2-syntrophin, thereby weakening its interaction with ICA512-TMF and promoting insulin secretion. Here we show that dissociation of the ICA512-TMF·β2-syntrophin complex following granule exocytosis is further enhanced by Ca^{2+}/calpain-1-induced generation of ICA512-CCF, which binds to both ICA512-TMF and β2-syntrophin. Receptor tyrosine phosphatases can either exist as monomers or form homodimers upon binding of a ligand to their ectodomain (47, 48). In the specific case of ICA512, it is still unknown whether the protein is present on the granules primarily as a monomer or a dimer. Dis-

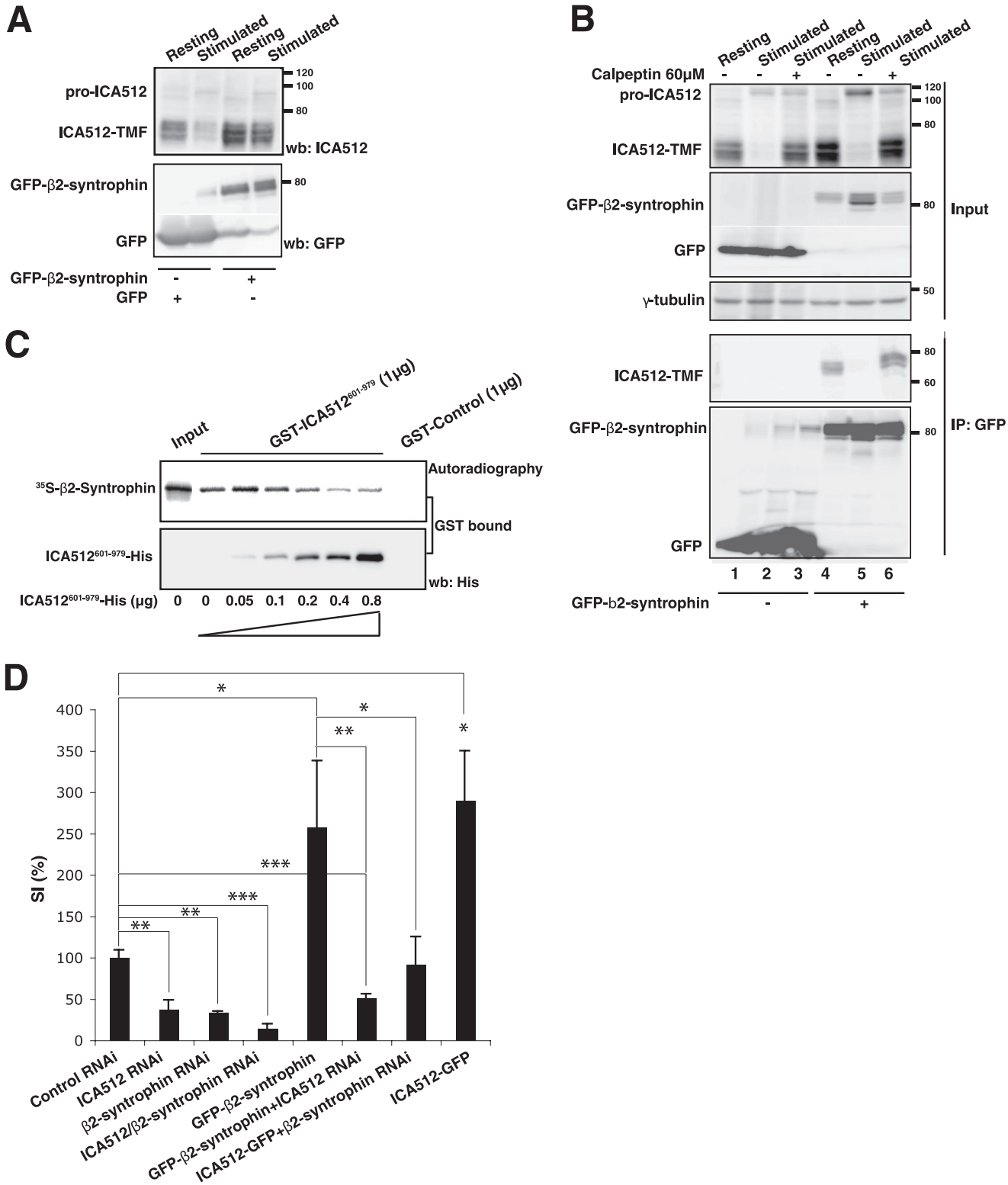

FIGURE 6. **ICA512-CCF dissociates ICA512-TMF from β2-syntrophin.** *A*, Western blots with mouse anti-ICA512 (*top*) or anti-GFP (*bottom*) antibodies on total protein extracts from resting or HGHK-stimulated INS-1 cells stably expressing GFP or GFP-β2-syntrophin. *B*, Western blots (*wb*) with mouse anti-ICA512 (*first* and *fourth panels* from the *top*), anti-GFP (*second* and *last panels* from the *top*), or anti-γ-tubulin (*third panel* from the *top*) antibodies on total protein extracts (*first three panels* from the *top*) or immunoprecipitates (*IP*) with anti-GFP antibodies from resting or HGHK-stimulated INS-1E cells. Cells were stably expressing GFP or GFP-β2-syntrophin and treated with or without 60 μM calpeptin. *C*, SDS-PAGE and autoradiography of *in vitro* transcribed and translated ^{35}S-labeled β2-syntrophin-His (*top*) and Western blot with anti-His antibody of bacterially expressed ICA512-(601–979)-His (*bottom*), pulled down with glutathione-Sepharose beads coupled to 1 μg of GST-ICA512-(601–979). *D*, SI from INS-1E cells transiently transfected with vectors for the individual or combined knockdown of *ICA512*, *β2-syntrophin*, or the control empty vector *pGENE-Clip* for RNA interference. Cells were co-transfected with 5 μg of mouse *GFP-β2-syntrophin* or human *ICA512-GFP*, as indicated. The SI in cells transfected with the empty vector equals 100%. The results are from at least three independent experiments performed in triplicate. *, $p < 0.05$; **, $p < 0.01$; ***, $p < 0.005$.

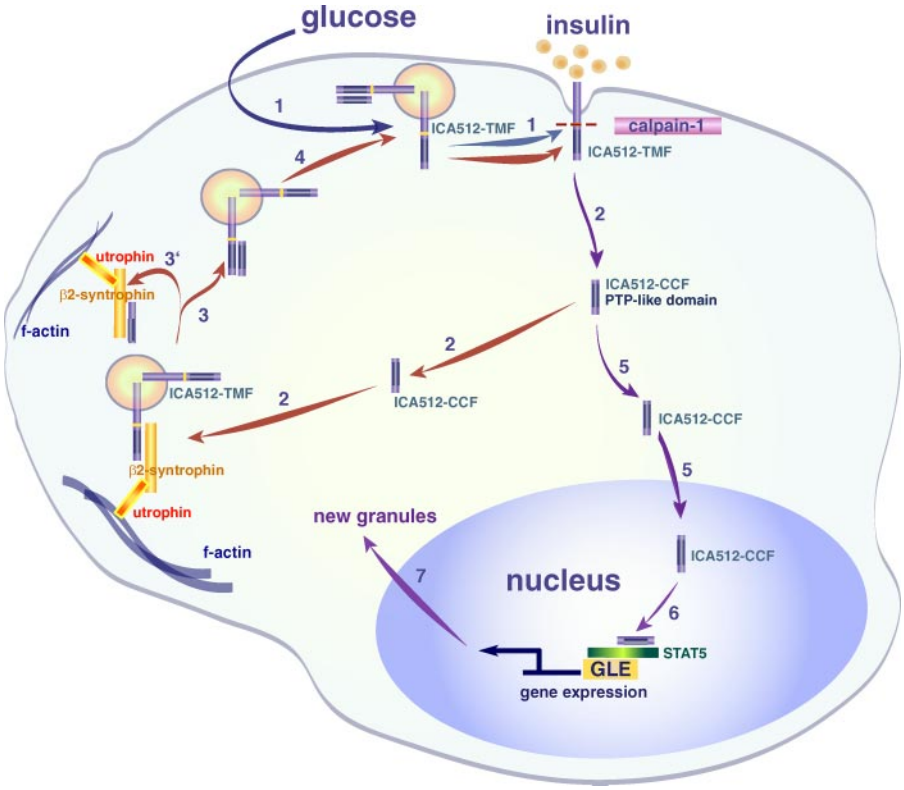

FIGURE 7. **Regulation of granule turnover by ICA512.** A schematic representation of a model illustrating how stimuli inducing the release of insulin, such as glucose (*1*), regulate granule turnover through the calpain-1-mediated cleavage of ICA512-TMF at the plasma membrane. The resulting cleaved cytoplasmic fragment, termed ICA512-CCF (*2*), disrupts the ICA512-TMF·β2-syntrophin complex by binding to either component of this complex (*3* and *3′*). The consequential displacement of granules from cortical actin increases their mobility and likelihood to approach sites competent for exocytosis (*4*). Progressive depletion of granules increases the probability that newly generated ICA512-CCF molecules reach the nucleus (*5*), thereby increasing the transcription of granule genes through the enhancement of STAT activity (*6*) and thus granule biogenesis (*7*). For graphic reasons, granules tethered to cortical actin filaments via the ICA512-TMF·β2-syntrophin complex were drawn distant from the plasma membrane, although in reality they are located in very close proximity to it.

placement of β2-syntrophin upon homodimerization of ICA512 suggests that β2-syntrophin only binds to monomeric ICA512.

The PDZ domain of β2-syntrophin is flanked on both sides by a split pleckstrin-homology domain, which in the case of α-syntrophin binds to $PI(4,5)P_2$. Generation of $PI(4,5)P_2$ at the plasma membrane is a critical step for the priming and release of secretory granules (49, 50). Binding of $PI(4,5)P_2$ to the pleckstrin homology domain of β2-syntrophin may affect the embedded PDZ domain and thus represent an additional means to modulate the interaction of ICA512 and the granules with cortical actin. In *Caenorhabditis elegans*, the *ICA512/IA-2* paralogue *CeIA-2/IDA-1* was shown to genetically interact with *UNC-31/CAPS*, an effector of $PI(4,5)P_2$ for granule priming and exocytosis (51, 52). Based on these considerations, it is tempting to speculate that the ICA512·β2-syntrophin complex is a hub where many distinct signals converge to modulate the interaction of granules with the cortical cytoskeleton.

Additional complexes regulating the interaction of insulin granules with the actin cytoskeleton and the cell cortex include the small GTPases Rab3a and Rab27a/b and their effectors Slac2c/MyRIP, Slp4/granuphilin, rabphilin-3a, Noc 2, and RIM (45, 53–56). Evidence that overexpression of ICA512-CCF results in unconstrained mobility of cortical granules suggests that these complexes tether granules to the cytoskeleton and the plasma membrane downstream of the ICA512·β2-syntrophin complex.

In summary, we propose a model whereby intracellular cleavage of ICA512-TMF in proportion to granule exocytosis originates a short feedback loop that amplifies insulin secretion by increasing granule mobility and hence their probability of encountering membrane sites competent for exocytosis (Fig. 7). Progressive depletion of granules, in turn, enhances the probability that ICA512-CCF reaches the nucleus, where it promotes transcription of granule genes, including insulin, as well as β-cell proliferation (26). This mechanism would allow β-cells to adjust their insulin production based on the size of the existing granule stores and their consumption in order to fulfill metabolic demand.

Acknowledgments—We thank M.-S. Lee for providing the ICA512$^{-/-}$ mice; M. E. Adams, K. Anastassiadis, D. Drechsel, G. Felsenfeld, S. Froehner, W. Huttner, M. Suchanek, and C. Thiele for reagents; F. Ehehalt, M. Jäger, and S. Munsche for help with islet isolation; J. Ouwendijk for generation of chromogranin B-mRFP1 INS-1 cells; S. Diez and B. Schott-Diez for help with TIRFM; P. De Camilli and M. Meyer-Hermann for reading the manuscript; S. Fullerton and members of the Solimena laboratory for discussion; L. Rohde for editing; and K. Pfriem and R. Liedtke for secretarial assistance.

REFERENCES

1. Zimmet, P., Alberti, K. G., and Shaw, J. (2001) *Nature* **414,** 782–787
2. Diamond, J. (2003) *Nature* **423,** 599–602
3. Saltiel, A. R. (2001) *Cell* **104,** 517–529
4. Bratanova-Tochkova, T. K., Cheng, H., Daniel, S., Gunawardana, S., Liu, Y. J., Mulvaney-Musa, J., Schermerhorn, T., Straub, S. G., Yajima, H., and Sharp, G. W. (2002) *Diabetes* **51,** Suppl. 1, 83–90
5. Rorsman, P., and Renstrom, E. (2003) *Diabetologia* **46,** 1029–1045
6. Klenchin, V. A., and Martin, T. F. (2000) *Biochimie* (*Paris*) **82,** 399–407
7. Waselle, L., Gerona, R. R., Vitale, N., Martin, T. F., Bader, M. F., and Regazzi, R. (2005) *Mol. Endocrinol.* **19,** 3097–3106
8. Donelan, M. J., Morfini, G., Julyan, R., Sommers, S., Hays, L., Kajio, H.,

Briaud, I., Easom, R. A., Molkentin, J. D., Brady, S. T., and Rhodes, C. J. (2002) *J. Biol. Chem.* **277,** 24232–24242
9. Ivarsson, R., Jing, X., Waselle, L., Regazzi, R., and Renstrom, E. (2005) *Traffic* **6,** 1027–1035
10. Varadi, A., Ainscow, E. K., Allan, V. J., and Rutter, G. A. (2002) *J. Cell Sci.* **115,** 4177–4189
11. Varadi, A., Tsuboi, T., and Rutter, G. A. (2005) *Mol. Biol. Cell* **16,** 2670–2680
12. Bruun, T. Z., Hoy, M., and Gromada, J. (2000) *Eur. J. Pharmacol.* **403,** 221–224
13. Li, G., Rungger-Brandle, E., Just, I., Jonas, J. C., Aktories, K., and Wollheim, C. B. (1994) *Mol. Biol. Cell* **5,** 1199–1213
14. Tomas, A., Yermen, B., Min, L., Pessin, J. E., and Halban, P. A. (2006) *J. Cell Sci.* **119,** 2156–2167
15. Waselle, L., Coppola, T., Fukuda, M., Iezzi, M., El-Amraoui, A., Petit, C., and Regazzi, R. (2003) *Mol. Biol. Cell* **14,** 4103–4113
16. Ort, T., Maksimova, E., Dirkx, R., Kachinsky, A. M., Berghs, S., Froehner, S. C., and Solimena, M. (2000) *Eur. J. Cell Biol.* **79,** 621–630
17. Ort, T., Voronov, S., Guo, J., Zawalich, K., Froehner, S. C., Zawalich, W., and Solimena, M. (2001) *EMBO J.* **20,** 4013–4023
18. Solimena, M., and Gerdes, H. H. (2003) *Trends Cell Biol.* **13,** 399–402
19. Drake, P. G., Peters, G. H., Andersen, H. S., Hendriks, W., and Moller, N. P. (2003) *Biochem. J.* **373,** 393–401
20. Lan, M. S., Lu, J., Goto, Y., and Notkins, A. L. (1994) *DNA Cell Biol.* **13,** 505–514
21. Rabin, D. U., Pleasic, S. M., Shapiro, J. A., Yoo-Warren, H., Oles, J., Hicks, J. M., Goldstein, D. E., and Rae, P. M. (1994) *J. Immunol.* **152,** 3183–3188
22. Solimena, M., Dirkx, R., Jr., Hermel, J. M., Pleasic-Williams, S., Shapiro, J. A., Caron, L., and Rabin, D. U. (1996) *EMBO J.* **15,** 2102–2114
23. Zahn, T. R., Macmorris, M. A., Dong, W., Day, R., and Hutton, J. C. (2001) *J. Comp. Neurol.* **429,** 127–143
24. Albrecht, D. E., and Froehner, S. C. (2002) *Neurosignals* **11,** 123–129
25. Mziaut, H., Kersting, S., Knoch, K. P., Fan, W. H., Trajkovski, M., Erdmann, K., Bergert, H., Ehehalt, F., Saeger, H. D., and Solimena, M. (2008) *Proc. Natl. Acad. Sci. U. S. A.* **105,** 674–679
26. Mziaut, H., Trajkovski, M., Kersting, S., Ehninger, A., Altkruger, A., Lemaitre, R. P., Schmidt, D., Saeger, H. D., Lee, M. S., Drechsel, D. N., Muller, S., and Solimena, M. (2006) *Nat. Cell Biol.* **8,** 435–445
27. Trajkovski, M., Mziaut, H., Altkruger, A., Ouwendijk, J., Knoch, K. P., Muller, S., and Solimena, M. (2004) *J. Cell Biol.* **167,** 1063–1074
28. Saeki, K., Zhu, M., Kubosaki, A., Xie, J., Lan, M. S., and Notkins, A. L. (2002) *Diabetes* **51,** 1842–1850
29. Harashima, S., Clark, A., Christie, M. R., and Notkins, A. L. (2005) *Proc. Natl. Acad. Sci. U. S. A.* **102,** 8704–8709
30. Gotoh, M., Maki, T., Kiyoizumi, T., Satomi, S., and Monaco, A. P. (1985) *Transplantation* **40,** 437–438
31. Merglen, A., Theander, S., Rubi, B., Chaffard, G., Wollheim, C. B., and Maechler, P. (2004) *Endocrinology* **145,** 667–678
32. Wang, H., and Iynedjian, P. B. (1997) *Proc. Natl. Acad. Sci. U. S. A.* **94,** 4372–4377
33. Asfari, M., Janjic, D., Meda, P., Li, G., Halban, P. A., and Wollheim, C. B. (1992) *Endocrinology* **130,** 167–178
34. Kachinsky, A. M., Froehner, S. C., and Milgram, S. L. (1999) *J. Cell Biol.* **145,** 391–402
35. Anastassiadis, K., Kim, J., Daigle, N., Sprengel, R., Scholer, H. R., and Stewart, A. F. (2002) *Gene* (*Amst.*) **298,** 159–172
36. Campbell, R. E., Tour, O., Palmer, A. E., Steinbach, P. A., Baird, G. S., Zacharias, D. A., and Tsien, R. Y. (2002) *Proc. Natl. Acad. Sci. U. S. A.* **99,** 7877–7882
37. Hermel, J. M., Dirkx, R., Jr., and Solimena, M. (1999) *Eur. J. Neurosci.* **11,** 2609–2620
38. Rink, J., Ghigo, E., Kalaidzidis, Y., and Zerial, M. (2005) *Cell* **122,** 735–749
39. Steiner, D. F., Chan, S. J., and Rubenstein, A. H. (2001) in *Handbook of Physiology*, Vol. II (Jefferson, L. S., Cherrington, A. D., and Goodman, H. M., eds) pp. 49–78, Oxford University Press, Inc., New York
40. Magistrelli, G., Toma, S., and Isacchi, A. (1996) *Biochem. Biophys. Res. Commun.* **227,** 581–588
41. Pouli, A. E., Emmanouilidou, E., Zhao, C., Wasmeier, C., Hutton, J. C., and Rutter, G. A. (1998) *Biochem. J.* **333,** 193–199
42. Huet, S., Karatekin, E., Tran, V. S., Fanget, I., Cribier, S., and Henry, J. P. (2006) *Biophys. J.* **91,** 3542–3559
43. Gross, S., Blanchetot, C., Schepens, J., Albet, S., Lammers, R., den Hertog, J., and Hendriks, W. (2002) *J. Biol. Chem.* **277,** 48139–48145
44. Kim, S. J., Jeong, D. G., Jeong, S. K., Yoon, T. S., and Ryu, S. E. (2007) *Diabetes* **56,** 41–48
45. Shibasaki, T., Sunaga, Y., Fujimoto, K., Kashima, Y., and Seino, S. (2004) *J. Biol. Chem.* **279,** 7956–7961
46. Olsen, J. V., Blagoev, B., Gnad, F., Macek, B., Kumar, C., Mortensen, P., and Mann, M. (2006) *Cell* **127,** 635–648
47. Chin, C. N., Sachs, J. N., and Engelman, D. M. (2005) *FEBS Lett.* **579,** 3855–3858
48. Majeti, R., Bilwes, A. M., Noel, J. P., Hunter, T., and Weiss, A. (1998) *Science* **279,** 88–91
49. Gong, L. W., Di Paolo, G., Diaz, E., Cestra, G., Diaz, M. E., Lindau, M., De Camilli, P., and Toomre, D. (2005) *Proc. Natl. Acad. Sci. U. S. A.* **102,** 5204–5209
50. Hay, J. C., Fisette, P. L., Jenkins, G. H., Fukami, K., Takenawa, T., Anderson, R. A., and Martin, T. F. (1995) *Nature* **374,** 173–177
51. Cai, T., Fukushige, T., Notkins, A. L., and Krause, M. (2004) *J. Neurosci.* **24,** 3115–3124
52. Loyet, K. M., Kowalchyk, J. A., Chaudhary, A., Chen, J., Prestwich, G. D., and Martin, T. F. (1998) *J. Biol. Chem.* **273,** 8337–8343
53. Cheviet, S., Waselle, L., and Regazzi, R. (2004) *Trends Cell Biol.* **14,** 525–528
54. Fukuda, M. (2006) *Biochem. Soc. Trans.* **34,** 691–695
55. Kasai, K., Ohara-Imaizumi, M., Takahashi, N., Mizutani, S., Zhao, S., Kikuta, T., Kasai, H., Nagamatsu, S., Gomi, H., and Izumi, T. (2005) *J. Clin. Invest.* **115,** 388–396
56. Shibasaki, T., and Seino, S. (2005) *Methods Enzymol.* **403,** 408–419